Accepted Manuscript

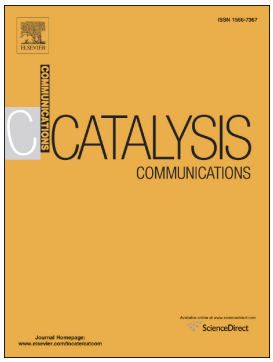

m-Cresol methylation: Role of internal and external acid sites in the product distribution

M.D. Acevedo, M.K. Montañez-Valencia, N.B. Okulik, M.E. Sad, C.L. Padró

PII: S1566-7367(16)30478-2
DOI: doi: 10.1016/j.catcom.2016.12.025
Reference: CATCOM 4894

To appear in: *Catalysis Communications*

Received date: 4 October 2016
Revised date: 19 December 2016
Accepted date: 20 December 2016

Please cite this article as: M.D. Acevedo, M.K. Montañez-Valencia, N.B. Okulik, M.E. Sad, C.L. Padró , m-Cresol methylation: Role of internal and external acid sites in the product distribution. The address for the corresponding author was captured as affiliation for all authors. Please check if appropriate. Catcom(2016), doi: 10.1016/j.catcom.2016.12.025

This is a PDF file of an unedited manuscript that has been accepted for publication. As a service to our customers we are providing this early version of the manuscript. The manuscript will undergo copyediting, typesetting, and review of the resulting proof before it is published in its final form. Please note that during the production process errors may be discovered which could affect the content, and all legal disclaimers that apply to the journal pertain.

ACCEPTED MANUSCRIPT

m-Cresol methylation: role of internal and external acid sites in the product distribution

M. D. Acevedo[1], M.K. Montañez-Valencia[2], N. B. Okulik[1], M.E.Sad[2], C.L. Padró[2*]

[1] *Universidad Nacional del Chaco Austral, Comandante Fernández 755, CP 3700, Pcia. Roque Sáenz Peña, Chaco, Argentina.*

[2]*Catalysis Science and Engineering Research Group (GICIC)*

Instituto de Investigaciones en Catálisis y Petroquímica -INCAPE-(UNL-CONICET)

Santiago del Estero 2654, (3000) Santa Fe, Argentina.

*** Corresponding author**

Prof. Cristina Padró
INCAPE, Santiago del Estero 2654
(3000) Santa Fe, Argentina
Email: cpadro@fiq.unl.edu.ar
Website: www.fiq.unl.edu.ar/gicic

ACCEPTED MANUSCRIPT

ACCEPTED MANUSCRIPT

Abstract

The effect of the porous structure and the role of internal and external acid sites in product distribution in gas-phase alkylation of m-cresol with methanol were studied on zeolites HBEA, HZSM5 and HMCM22. Catalysts were characterized by N_2 physisorption and FTIR of adsorbed pyridine. Trimethylated product formation was inhibited in narrower pore size zeolites (HMCM22 and HZSM5) and a preferential selectivity to smallest dimethylphenol isomer (2,5-dimethylphenol) was observed. The selectivity to 2,5-dimethylphenol on HMCM22 reached a value of 82% after suppressing the acid sites of the external cavities and pore mouth using 2,4-dimethylquinoline, which is a basic molecule too bulky to diffuse through the narrow pores of these zeolites.

Keywords: m-Cresol alkylation; Shape selectivity; Zeolites

1. Introduction

Valuable products can be obtained by m-cresol methylation. Dimethyl-phenols (DMP) and 3 methyl-anisole (3-MA), may be produced by C-alkylation and O-alkylation of m-cresol, respectively (Scheme 1). In addition, trimethylphenols (TMP) and dimethylanisoles (DMA) could be formed by successive alkylation. Among the dimethylphenols, 2,3-DMP is used in pesticides production, 3,4-DMP is the raw material in the insecticide 3,4-dimethylphenyl methylcarbamate synthesis and 2,5-DMP is the starting material in the manufacture of pharmaceuticals such as gemfibrozil (an oral drug used to lower lipid levels) and is also an intermediate in synthesis of colorants,

ACCEPTED MANUSCRIPT

antiseptics and antioxidants. Nevertheless, if the reaction proceeds without selectivity control, a mixture of all these products is formed. Therefore, considerable effort has been made to find active and selective catalysts for this reaction. The use of catalysts basic, redox and acids, such as MgO, Mg/Me (Al, Fe, Cr)-mixed oxides, V_2O_5 and zeolites in m-cresol methylation, has been rather studied [1-8]. Basic and redox catalysts showed high chemo-selectivity producing only minor amount of O-alkylation product and also regio-selectivity, being the *ortho*-DMP isomer favored at temperatures between 628 K and 673 K [1,5,7]. However, under these conditions, particularly on redox catalysts like Mg/Cr/O, Mg/Fe/O or Fe/SiCr/O, methanol decomposed and it becomes necessary to feed this reactant in a large excess over the stoichiometric ratio.

The catalytic activity and selectivity of acid catalysts strongly depend on the nature and strength of the catalytic surface sites [8]. HBEA, which contains acid sites of Brønsted and Lewis nature of considerable strength, is fairly unselective forming O-alkyltion and C-alkylation products corresponding to C/O alkylation ratio of 1.9 while on Al-MCM-41 (mostly acid Lewis sites of moderate strength) the main product of reaction was 3-MA ($S_{3\text{-}MA}$=56%) giving a C/O-alkylation ratio of 0.72. C-methylation was selectively promoted by ZnY (C/O alkylation ratio: 8.8) that has strong Lewis acidity.

On another hand, the product distribution can also be modified by shape selectivity. Even though it has been claimed that zeolites (HY, HZSM5 and HBEA) that yielded p-xylene selectively in toluene methylation did not display shape selectivity in the alkylation of phenol with methanol [9], selective formation of p-cresol

ACCEPTED MANUSCRIPT

("slimmest" cresol isomer) have been reported on HMCM22 both in gas and liquid phase [10,11].

With the aim to control the product distribution, in this work we have studied the effect of porous structure and the role of internal and external acid sites on the product selectivities in m-cresol methylation. In this regard, we have tested in the reaction three zeolites (HBEA, HZSM5 and HMCM22) before and after poisoning with 2,4-dimethylquinoline (2,4-DMQ), which is a molecule too bulky to diffuse through the narrow pores of HZSM5 and HMCM22 zeolite [12-14]. These catalysts were selected for their particular pore structure. Zeolite HMCM22 contains independent pore systems: large supercages (18.2 × 7.1 × 7.1 Å) connected by 10-MR openings (4.0×5.5 Å), bidimensional sinusoidal channels (4.1 × 5.1 Å), and large external cups, corresponding to hemisupercages (7.0 ×7.1 × 7.1 Å). HZSM5 zeolite has a three-dimensional channel system with elliptical aperture (5.1 x 5.5 Å) interconnected by zigzag channels with approximately circular cross section of 5.3 x 5.6 Å with no cages. HBEA zeolite has straight channels (7.6 Å × 6.4 Å) interconnected through sinusoidal channels (diameter 5.6 Å). The channels intersections generate 12–13 Å cavities [15].

2. Experimental

2.1. Catalyst Preparation and Characterization

ACCEPTED MANUSCRIPT

Commercial sample of zeolite HZSM5 (Zeocat Pentasil PZ-2/54, Si/Al = 20) and HBEA (Zeocat PB/H, Si/Al=12.5) were used. Zeolite HMCM22 was synthesized according to method reported in the literature with a synthesis gel composition of SiO_2/Al_2O_3=30, $OH=SiO_2$=0.18, hexamethyleneimine/SiO_2=0.35 and H_2O/SiO_2=45 [16]. The three zeolites were calcined before use at 773 K in dry air (60 cm^3min^{-1}).

The external acid sites of HMCM22 and HZSM5 zeolites were poisoned with 2,4-dimethylquinoline (2,4-DMQ) by incipient wetness impregnation. Since 2,4-dimethylquinoline (2,4-DMQ) is not volatile enough to be introduced in the gas phase, the desired amount (1.225 mmol per gram of zeolite) of 2,4-DMQ was solubilized in methylene chloride. The solvent was eliminated by treating the poisoned samples (HMCM22p and HZSM5p) in flowing N_2 at 473 K during 0.5 h.

Total surface areas (S_{BET}) and sample porosities were measured by physisorption of N_2 at 77 K in a Autosorb Quantochrome Instrument 1-C sorptometer. Before N_2 adsorption, samples were treated under vacuum at 623 K for 8 h. The zeolite micropore volumes were determined using the adsorption branch of nitrogen isotherms by both Dubinin-Radushkevich [17] and *t*-plot [18] methods. The *t*-plot was obtained by using de Harkins-Jura equation [19]. The external surface areas (S_e), were obtained from the slopes of the *t*-plot lines.

Nature and strength of surface acid sites were studied by Infrared Spectroscopy (IR) using pyridine as a probe molecule in a Shimadzu FTIR Prestige-21 spectrophotometer. The samples were outgassed in vacuum at 723 K during 2 h and cooled to 298 K under evacuation. Spectra, average of 40 runs, were recorded at room temperature, after admission of pyridine, adsorption at room temperature and sequential evacuation at 373 K and 473 K. The resolution used in all experimentes was 4 cm^{-1}. The

ACCEPTED MANUSCRIPT

spectrum recorded after treatment and before pyridine adsorption was taking as a reference spectrum.

2.2. Catalytic activity

Gas phase methylation of m-cresol (Sigma-Aldrich, >98%) with methanol (Merck, 99.8%) was carried out using a fixed bed continuous flow reactor at 523 K and 101.3 kPa. Catalysts were treated in situ at 473 K in N_2 flow before reaction. The feed (m-cresol/methanol solution, molar ratio methanol/m-cresol=5) was introduced by means of a syringe pump (Cole-Parmer EW-74900) and vaporized in a preheated N_2 stream to give a N_2 / (m-cresol+methanol) ratio of 37. Reactants and products were analyzed on-line using an UNICAM 610 chromatograph equipped with a flame ionization detector and a 30 m Innowax column (inner diameter: 0.32 mm, film thickness: 0.5 μm). Main reaction products were dimethylphenols (2,5-, 2,3- and 3,4-DMP), 3-methylanisole (3-MA), trimethylphenols (TMP) and dimethylanisoles (DMA).

m-Cresol conversion ($X_{m\text{-}cresol}$) was calculated as: $X_{m\text{-}cresol}=(Y^0_{m\text{-}cresol}-Y_{m\text{-}cresol,})/Y^0_{m\text{-}cresol}$ where $Y^0_{m\text{-}cresol}$ is the molar fraction of m-cresol at the entrance of the reactor while $Y_{m\text{-}cresol}$ is the molar fraction at the exit. The selectivity to product *i* formed from m-cresol molecules (S_i, mol of product *i*/mol of m-cresol reacted) was determined as: $S_i = [Y_i/\Sigma Y_i]$ where Y_i is the molar fraction of products formed from m-cresol.

3. Results and Discussion

ACCEPTED MANUSCRIPT

3.1. Catalyst characterization

The physical and textural properties of the samples are presented in Table 1. BET surface area of HBEA (632 m^2g^{-1}) was higher than those determined for HMCM22 (400 m^2g^{-1}) and HZSM5 (350 m^2g^{-1}). The external surface areas, Se, obtained from the slope of the t-plot lines, were about 70 m^2g^{-1} for HZSM5 and HMCM22, substantially lower than that of HBEA (304 m^2g^{-1}). The zeolite micropore volumes (< 20 Å) determined by Dubinin–Radushkevich were slightly greater than those determined from t-plots. Both methods revealed that the micropore volumes of HMCM22 and HBEA were similar and higher than the value determined for HZSM5. In the case of zeolite HMCM22, the presence of ultramicropores (<6Å) was detected. Therefore, we also determined the ultramicropore volume of HMCM22 (0.10 cm^3g^{-1}). The pore volume determined here for HMCM22 is consistent with values reported in literature. [13, 20, 21].

The nature of surface acid sites were studied by FTIR after adsorption of pyridine at 298 K and evacuation at 373 K and 473 K. The concentrations of Brønsted and Lewis acid sites (C_B and C_L, μmol g^{-1}) after evacuation of pyridine at 373 K and 473 K were estimated from the area of the characteristic bands at 1540-1550 cm^{-1} (A_B) and 1440-1450 cm^{-1} (A_L). [22,23] using the equations derived by Emeis [24]. Results are included in Table 2.

FTIR spectra of the three zeolites revealed the presence of both Lewis (bands at 1455 cm^{-1} and 1620 cm^{-1}) and Brønsted acid sites (bands at 1540 cm^{-1} and 1635 cm^{-1}).

ACCEPTED MANUSCRIPT

After outgassing at 373 K, C_B/C_L ratios of 1.7, 1.4 and 4.6 were determined for zeolites HBEA, HZSM5 and HMCM22, respectively. Furthermore, the Py-473K/Py-373K ratios (i.e. the ratio of the amounts of pyridine remaining on the samples after evacuation at 473 K and 373 K) were 0.75, 0.87 and 0.83 on HBEA, HZSM5 and HMCM22, respectively, thereby indicating that these zeolites presented strong acid sites predominantly of Brønsted nature. It is worth noting that the concentration of Brønsted acid sites that retained pyridine following evacuation at 473 k is somewhat higher than after evacuation at 373 K, probably due to pyridine migration from some Lewis acid sites during the outgassing

IR spectra of pyridine adsorbed were also obtained on samples impregnated with 2,4-DMQ (HZSM5p and HMCM22p) after evaporating the solvent in N_2 flow and evacuation under vacuum at 473 K for 2 h. A significant drop in the concentration of Brønsted acid sites able to retain pyridine, comparing with samples without poisoning, was observed (Table 2). Meanwhile, Lewis acid concentrations changed just a little. In fact, C_B dropped almost to half in both zeolites after evacuation at 373K and fell 60% after desorption at 473K. 2,4 DMQ is a bulky base whose diffusion into the small channels that have both zeolites is hampered adsorbing only on external acid sites, furthermore, 2,4 DMQ cannot be adsorbed on Lewis sites by steric hindrance [12].

3.2. Catalytic results for methylation of m-cresol

Catalysts were tested in gas phase methylation of m-cresol at 523 K. In Fig. 1, we plotted the m-cresol conversion ($X_{m\text{-}cresol}$) and products selectivities (S_i) as a function of time obtained on HMCM22 using a contact time of $W/F^0_{m\text{-}Cresol}$ = 181 g h mol^{-1} as an example of typical time-on-stream behavior of the catalysts studied in this work. Main

ACCEPTED MANUSCRIPT

products formed were 3-MA and 2,5- 2,3- and 3,4-DMP. Selectivities did not change significantly during reaction, even though m-cresol conversion ($X_{m\text{-}cresol}$) decreased with time evidencing some deactivation on this catalyst. A clear preference to C-alkylation was noticed, maintaining $S_{3\text{-}MA}$ below 10% all the time.

In order to determine the relationship between the acidity (nature and strength of the acid sites) and porous structure with the product distribution formed by m-cresol methylation, we compare the selectivities on fresh catalysts at a same m-cresol conversion level, testing the catalysts at different contact times (keeping unmodified the rest of the reaction conditions). Results at $X^0_{m\text{-}cresol}$=20% are plotted in Figure 2. Formation of TMP (products of the C-methylation of DMP) and DMA (from C-alkylation of 3-MA or O-alkylation of DMP) was scarce, especially on HMCM22 and HZSM5 what may be due to their narrow pore structures that prevent the formation of the bulky intermediates involved [25]. The highest C/O-alkylation value (13.3) was obtained on HMCM22, zeolite with strong acid sites and higher C_B/C_L ratio followed by HZSM5 (2.5) and HBEA (1.9) confirming that the selectivity to the C-alkylation at this temperature depends primarily on the strength of the acid sites [8,10].

About the DMP isomers, the products of electrophilic substitution on favored *ortho*- and *para*- positions: 2,3-, 2,5- and 3,4-DMP were formed in similar amounts on HBEA, however, the isomers distribution was markedly different from statistical (Figure 2) on the zeolites with narrower pores. A preferential formation of one of *ortho*-alkylation product, 2,5-DMP, was observed, giving rise a *ortho/para* ratios of 3.7 and 2.5 on HZSM5 and HMCM22 zeolites, respectively. In particular on HZSM5 the selectivity to 2,5-DMP was 49%, as shown in Figure 2, corresponding to 69% of DMP formed. In literature there

ACCEPTED MANUSCRIPT

is little information concerning the isomer distribution on acid catalysts, however it has been reported that on Al-MCM-41 and zeolites HY an *ortho/para*-C-methylation ratio close to statistical (*o/p* = 2), was obtained in both liquid and gas phase [6,8].

Additional experiences at different contact times ($W/F^0_{m-cresol}$) on HZSM5 were performed. In Figure 3 the selectivities as a function of m-cresol conversion at t=0 are plotted. It is noted that increasing conversion, S_{3MA} decreases probably due to a secondary reaction of formation of DMP from 3-MA reported previously by other authors [5]. Among DMP isomers, 2,5-DMP selectivity increases, while selectivity to 2,3-DMP decreases and 3,4-DMP remains practically invariant. Moreover, the growth in conversion produced only a small rise in selectivity to secondary products, mainly trimethylphenols (S_{TMP} =6.1% for $X^0_{m\text{-}cresol}$=57%). This, as mentioned previously, may be due to diffusional limitation in the small channels of this material. In fact, in the alkylation of phenol with methanol at 473 K on this catalyst trimethylated products are not formed [25].

It is remarkable the high $S_{2,5\text{-}DMP}$ (57% at $X^0_{m\text{-}cresol}$= 57%) and a likely explanation is the existence of shape selectivity in HZSM5 zeolite. Comparing the relative dimensions of the isomers: 2,5-DMP, 2,3-DMP and 3,4-DMP (Fig. 4), we might speculate that 2,5-DMP would diffuse at higher rate than the other isomers inside the narrow channels of this zeolite. However, it has to be noted that it was not observed the same effect on HMCM22. Opposed results have been reached for phenol methylation [25] where p-Cresol (smallest cresol isomer) was selectively synthetized on HMCM22, while on HZSM5 the selectivity to p-cresol was not improved, even though product from over alkylation (DMP or TMP) formation was hampered on both catalysts by diffusional constraints.

ACCEPTED MANUSCRIPT

Considering that the acid sites located in the external cavities of HMCM22 have been claimed to be more active or even the only ones involved in certain reactions [13], catalytic experiments with samples HZSM5 and HMCM22 whose outer surface has been poisoned with 2,4-DMQ were carried out. This basic molecule was selected since, besides being too bulky to enter inside the small channels, slightly volatile and is expected to remain adsorbed even at reaction conditions. In previous works, 2,4-DMQ has been used as a poison to deactivate the outer surface during reaction both on HZSM5 [14] as on HMCM22 [12, 13]. Although it was stated that 2,4-DMQ only poisons external acid sites of HZSM5, decreasing the activity 25% in the p-xylene isomerization, on HMCM22 it has been proved by FTIR that 2,4-DMQ can be adsorbed not only on the acid sites located in the external cavities but also in the sinusoidal channels, probably in pore mouth area, and it may diffuse in some extent to the inner with time and high temperature [12].

The results of catalytic test on poisoned samples (HMCM22p and HZSM5p) are shown in Figure 5. We have also added the selectivities on samples without poisoning at same level of conversion ($X^0_{\text{m-cresol}}$=10%) for proper comparison.

On both zeolites the selectivity to smallest DMP isomer (2,5-DMP) was improved by deactivating external sites supporting its formation within the channels of both zeolites. This effect of shape selectivity is more noticeable on HMCM22 since it has smaller pores reaching $S_{2,5\text{-DMP}}$ = 82%. On HZSM5, after being poisoned with 2.4-DMQ, selectivity to 2,5-DMP and to the isomer following in size, 3,4-DMP, were increased at the expense of 3-MA and 2,3-DMP. Additionally the formation of TMP, although small in the sample without poisoning, was canceled out completely proving that the bulkier molecules could only be formed on the outer surface of the zeolite.

ACCEPTED MANUSCRIPT

4. Conclusions

In this work, the effect of the porous structure and the role of internal and external acid sites of three zeolites in product distribution was studied in gas phase methylation of m-cresol. It was observed that trimethylated product formation was inhibited in smaller pore size zeolites (HMCM22 and HZSM5) and additionally a preferential selectivity to smallest dimethylphenol isomer (2,5-DMP) was observed. The product selectivity on HMCM22 increased to 82% by supressing the acid sites of the external cavities and pore mouth using 2,4-dimethylquinoline (2,4-DMQ), which is a basic molecule too bulky to diffuse through the narrow pores of these zeolites.

5. Acknowledgments

This work was supported by the Universidad Nacional del Litoral (UNL), Universidad Nacional del Chaco Austral (UNCAUS), Consejo Nacional de Investigaciones Científicas y Técnicas (CONICET), and Agencia Nacional de Promoción Científica y Tecnológica (ANPCyT), Argentina.

6. References

[1] Grabowska, H., Wrzyszcz, J., Syper, L. Catal. Lett. 57 (1999) 135 -137

[2] Durgakumari, V., Narayana, S. J. of Molec. Catal. 65 (1991) 385-392

[3] Durgakumari, V., Sreekanth G., Narayanan, S. Res. Chem. Intermed. 14 (1990) 223-233.

[4] Bolognini, M., Cavani, F., Scagliarini, D., Flego, C., Perego, C., Saba, M., Catal. Today 75 (2002) 103-111

ACCEPTED MANUSCRIPT

[5] Crocella, V., Cerrato, G., Magnacca, G., Morterra, C., Cavani, F., Cocchi, S., Passeri, S., Scagliarini, D., Flego, C., Perego, C., J. of Catal. 270 (2010) 125-135

[6] Cavani, F., Maselli, L., Scagliarini, D., Flego, C., Perego, C. in Gamba, A. Colella, C., Coluccia, S. (eds.) Stud. in Surf. Sci. and Catal. 155 (2005) 167-177

[7] Crocellà, V, Cerrato, G., Magnacca, G. Morterra, C., Cavani, F.L. Maselli, L. Passeri, S. Dalton Trans.39 (2010) 8527-8537

[8] Acevedo, M.D., Bedogni, G.A., Okulik, N.B., Padró, C.L. Catal Lett 144-11 (2014) 1946-1954

[9] Landau, M.V. Kogan S.B., Tavor D., Herskowitz M., Koresh J.E. Catalysis Today 36 (1997) 497-510

[10] Sad, M.E., Padró, C.L., Apesteguía, C.R., Appl. Catal. A 342 (2008) 40-48

[11] Moon G., Böhringer, W. O'Connor, C.T., Catal. Today 97 (2004) 291-295.

[12] Ayrault, P., Datka, J., Laforge, S., Martin, D., Guisnet M., J. Phys.Chem. B 108 (2004) 13755-13763

[13] Rigoreau, J. Laforge, S. Gnep, N.S. Guisnet, M., J. Catal. 236 (2005) 45–54

[14] Namba, S., Nakanishi, S., Yashima, T. J. Catal. 88 (1984) 505-508

[15] Benslama, R. J. Fraissard, J. Albizane, A. Fajula, F. Figueras, F. Zeolites 8-3 (1988) 196-198

[16] Rubin, M.K., Chu, P. , (1990) US Patent 4.954.325

[17] Dubinin, M.M., Radushkevich, L.V. Dokl. Akad. Nauk. SSSR 55 (1947) 331-337.

[18] Lippens, B.C., Linsen, B.G, De Boer, J.H., J. Catal. 3 (1964) 32-37.

[19] W.D. Harkins, G. Jura, J. Chem. Phys. 11 (1943) 431-432.

[20] Juttu, G.G., Lobo, R.F., Micropor. Mesopor. Mater. 40 (2000) 9-23.

[21] Meloni, D. Laforge, S. Martin, D. Guisnet M., Rombi, E. Solinas, V., Appl. Catal. A: General 215 (2001) 55-66.

[22] Parry, E.P., J. Catal. 2 (1963) 371-379

[23] Busca, G. Catal. Today 41 (1998) 191-206

[24] Emeis, C.A. J. Catal. 141 (1993) 347-354

[25] Sad, M.E., Padró, C.L., Apesteguía, C.R., Appl. Catal. A 342 (2008) 40-48

ACCEPTED MANUSCRIPT

ACCEPTED MANUSCRIPT

ACCEPTED MANUSCRIPT

Table 1: Textural properties of the catalysts

Catalysts	S_{BET} (m^2g^{-1})	*t*-plot method			Dubinin-Radushkevich method
		Micropore volumen (cm^3g^{-1})	Ultramicropore volume (cm^3g^{-1})	External surface area S_e (m^2g^{-1})	Micropore volumen (cm^3g^{-1})
HBEA	632	0.168	-	304	0.24
HZSM5	350	0.155	-	73	0.18
HMCM22	400	0.169	0.10	68	0.21

ACCEPTED MANUSCRIPT

ACCEPTED MANUSCRIPT

Table 2. FTIR of Pyridine.

Zeolite	**$T_{desorption}$=373 K**		**$T_{desorption}$=473 K**	
	Lewis concentration (C_L) (**μ**mol g^{-1})	Brønsted concentration (C_B) (**μ**mol g^{-1})	Lewis concentration (C_L) (**μ**mol g^{-1})	Brønsted concentration (C_B) (**μ**mol g^{-1})
HBEA	185	307	73	295
HZSM5	213	300	100	335
HZSM5p	210	141	95	135
HMCM22	91	410	74	345
HMCM22p	93	213	83	136

ACCEPTED MANUSCRIPT

ACCEPTED MANUSCRIPT

Figure Captions

Scheme 1: Reaction network for methylation of m-cresol on solid acids.

Figure 1: m-Cresol conversion ($X_{m\text{-}Cresol}$) and Selectivities (S_i) as a function of time-on-stream on HMCM22 [523 K, P_T=101.3 kPa, W/F_P^0 = 181 g h mol^{-1} , $P_{m\text{-}cresol}$=0.44 kPa, $P_{methanol}$=2.23 kPa].

$X_{m\text{-}Cresol}$ (O),S_{3MA} (●), $S_{2,5DMP}$ (■),$S_{2,3DMP}$ (□),$S_{3,4DMP}$ (◆),S_{DMA} (▼), S_{TMP} (▽)

Figure 2: Selectivities (S_i^0, %) compared at same level of m-Cresol conversion on fresh catalysts

[523 K, P_T=101.3 kPa, $P_{m\text{-}cresol}$=0.44 kPa, $P_{methanol}$=2.23 kPa, $X^0_{m\text{-}cresol} \cong$ 20%].

Figure 3: Selectivities (S_i^0, %) as a function of m-cresol conversion ($X^0_{m\text{-}cresol}$) at t=0 for HZSM5 [523 K, P_T=101.3 kPa, $P_{m\text{-}cresol}$=0.44 kPa, $P_{methanol}$=2.23 kPa].

S_{3MA} (●), $S_{2,5DMP}$ (■),$S_{2,3DMP}$ (□),$S_{3,4DMP}$ (◆),S_{DMA} (▼), S_{TMP} (▽)

Figure 4: Schematic representation of 2,3-DMP, 2,5-DMP and 3,4-DMP

ACCEPTED MANUSCRIPT

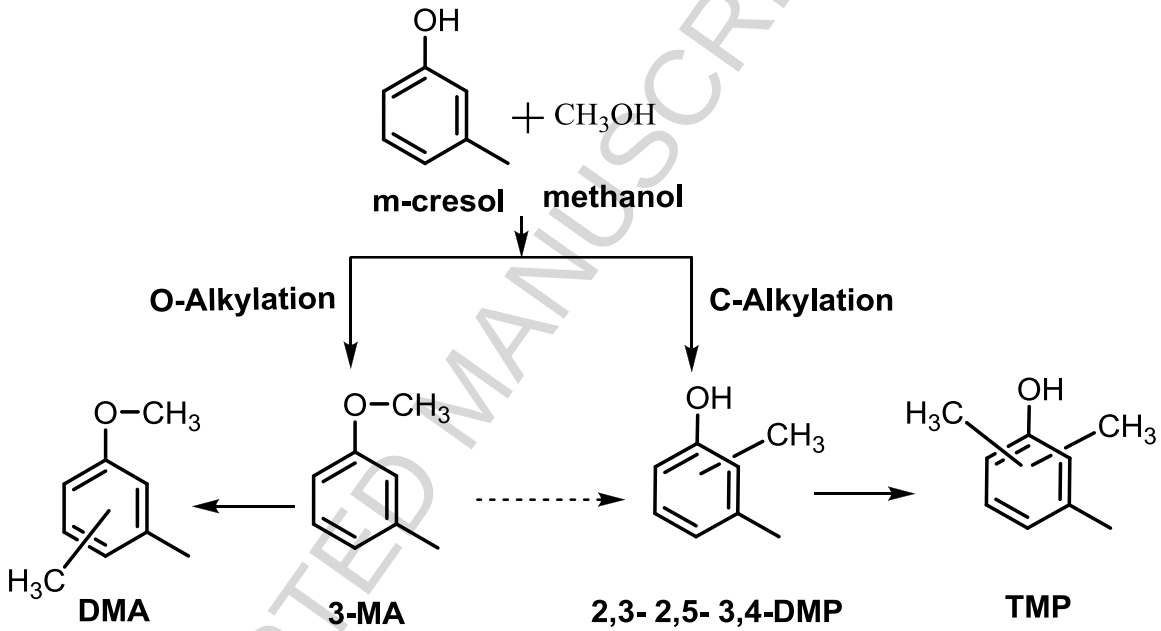

Scheme 1: Reaction network for methylation of m-cresol on solid acids.

ACCEPTED MANUSCRIPT

ACCEPTED MANUSCRIPT

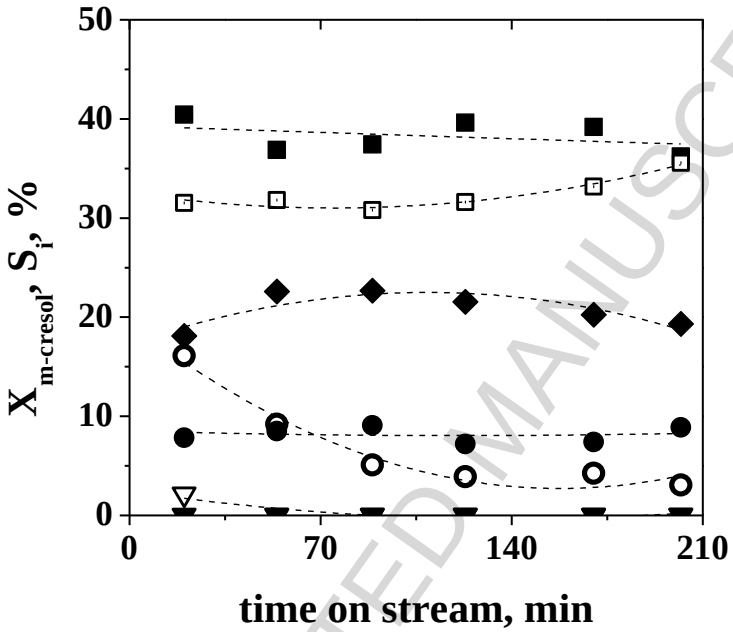

Figure 1: m-Cresol conversion ($X_{m\text{-}Cresol}$) and Selectivities (S_i) as a function of time-on-stream on HMCM22 [523 K, P_T=101.3 kPa, W/F_P^0 = 181 g h mol^{-1}, $P_{m\text{-}cresol}$=0.44 kPa, $P_{methanol}$=2.23 kPa].

$X_{m\text{-}Cresol}$ (○),S_{3MA} (●), $S_{2,5DMP}$ (■),$S_{2,3DMP}$ (□),$S_{3,4DMP}$ (◆),S_{DMA} (▼), S_{TMP} (▽)

ACCEPTED MANUSCRIPT

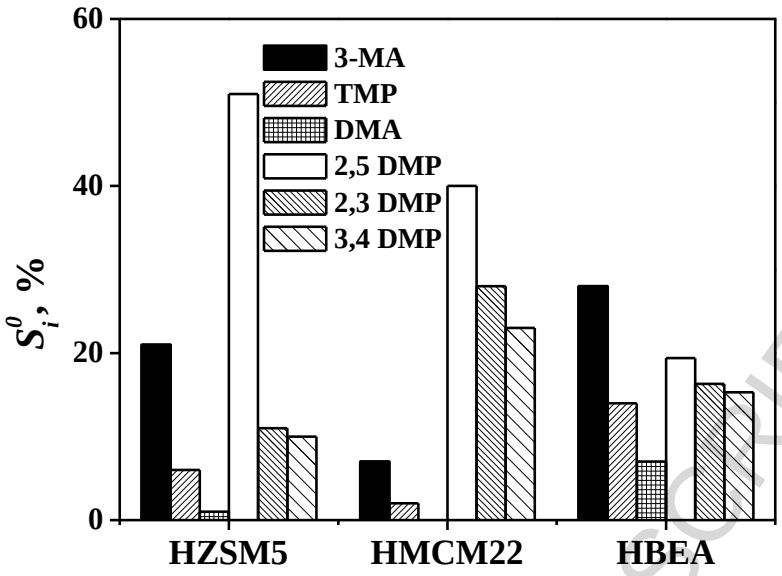

Figure 2: Selectivities (S_i^0, %) compared at same level of m-Cresol conversion on fresh catalysts

[523 K, P_T=101.3 kPa, $P_{m\text{-}cresol}$=0.44 kPa, $P_{methanol}$=2.23 kPa, $X^0_{m\text{-}cresol} \cong$ 20%].

ACCEPTED MANUSCRIPT

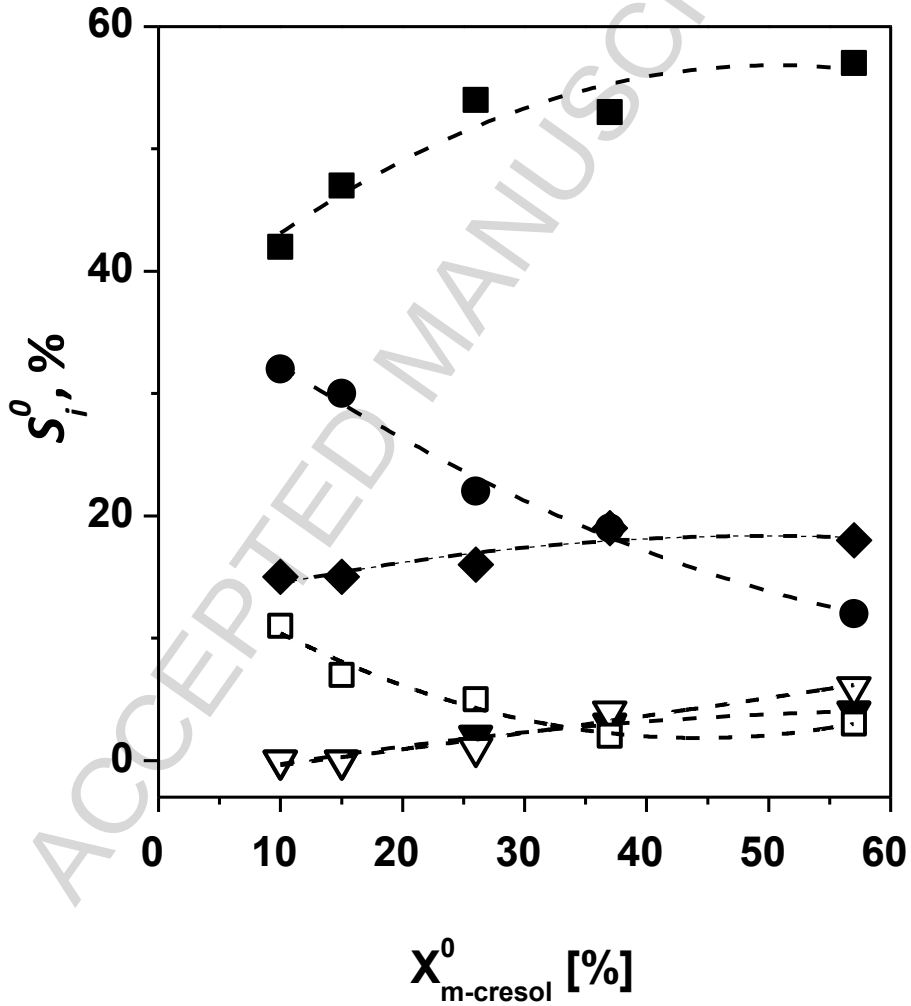

Figure 3: Selectivities (S_i^0, %) as a function of m-cresol conversion ($X^0_{m\text{-}cresol}$) at t=0 for HZSM5 [523 K, P_T=101.3 kPa, $P_{m\text{-}cresol}$=0.44 kPa, $P_{methanol}$=2.23 kPa].

S_{3MA} (●), $S_{2,5DMP}$ (■),$S_{2,3DMP}$ (□),$S_{3,4DMP}$ (◆),S_{DMA} (▼), S_{TMP} (▽)

ACCEPTED MANUSCRIPT

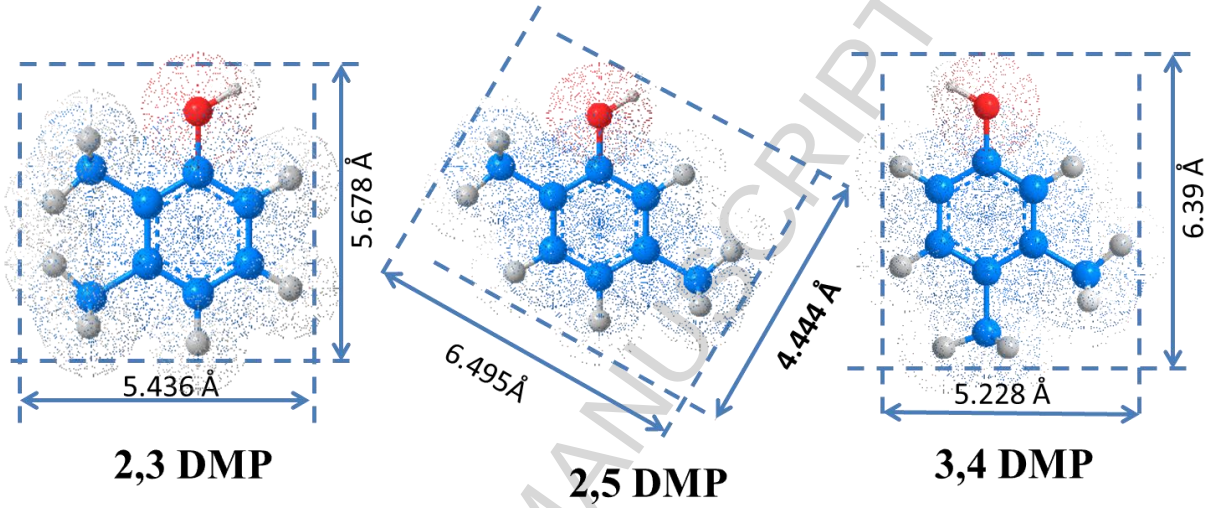

Figure 4: Schematic representation of 2,3-DMP, 2,5-DMP and 3,4-DMP

ACCEPTED MANUSCRIPT

ACCEPTED MANUSCRIPT

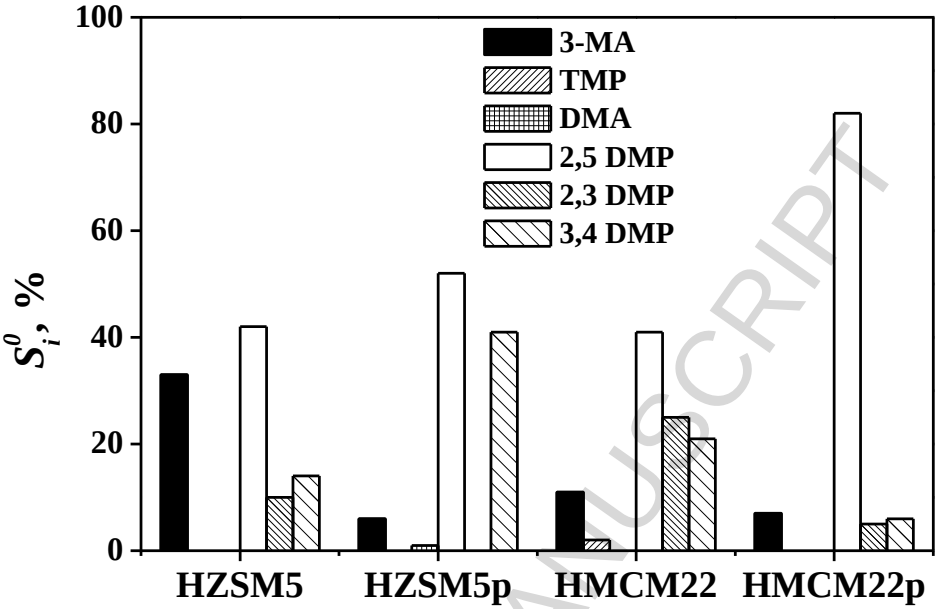

Figure 5 : Selectivities (S_i^0, %) compared at same level of m-Cresol conversion at t=0 on poisoned and not poisoned catalysts

[523 K, P_T=101.3 kPa, $P_{m\text{-}cresol}$=0.44 kPa, $P_{methanol}$=2.23 kPa, $X^0_{m\text{-}cresol} \cong$ 10%].

ACCEPTED MANUSCRIPT

ACCEPTED MANUSCRIPT

Graphical Abstract

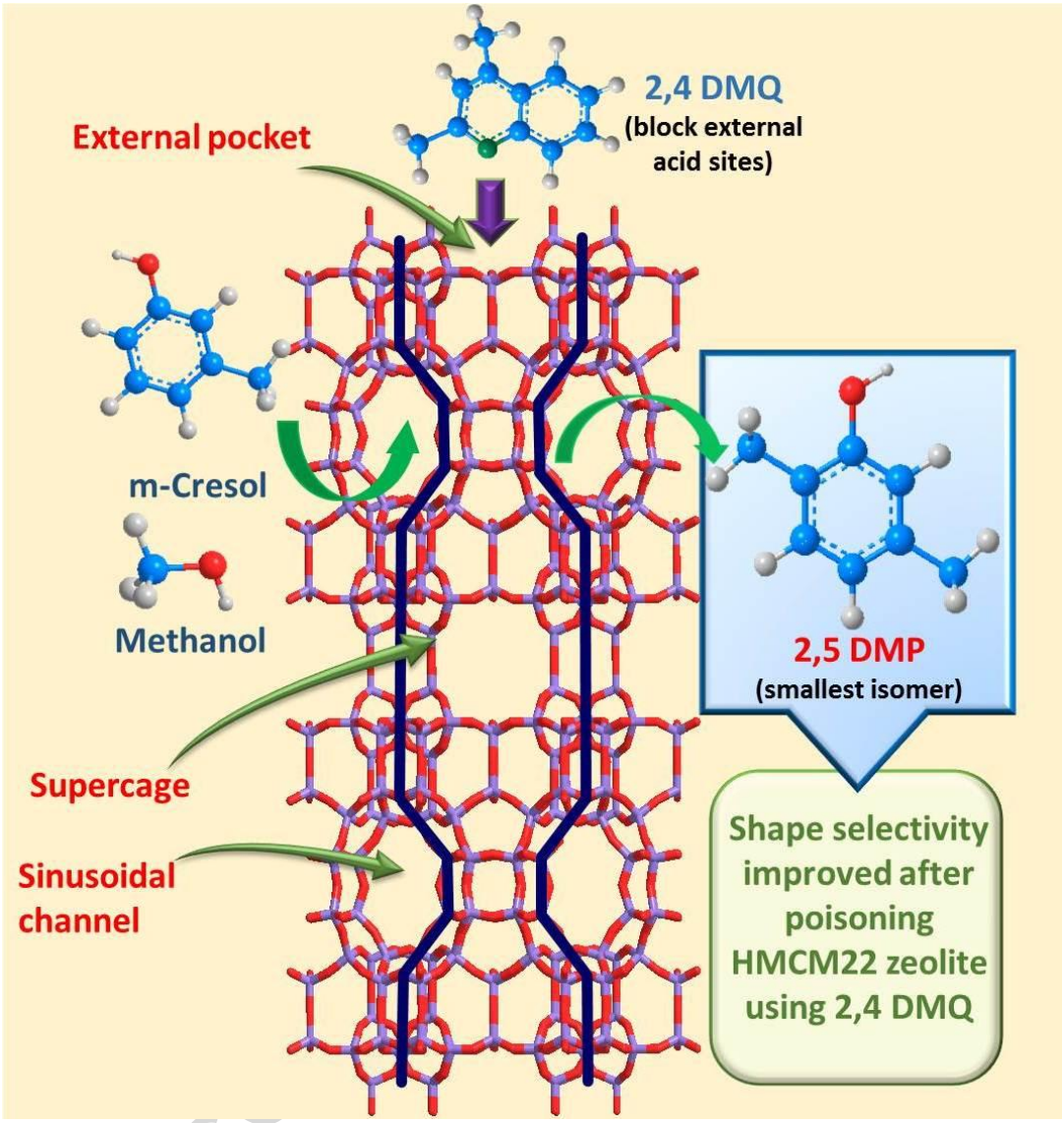

ACCEPTED MANUSCRIPT

Highlights

1. m-Cresol methylation was studied over HBEA, HZSM5 and HMCM22
2. Selectivity can be modified by shape selectivity
3. High selectivity to 2,5-DMP can be achieved in the narrow pores of HMCM22

ACCEPTED MANUSCRIPT